Millimeter-Wave Planar InP Schottky Diodes and Their Small-Signal Equivalent Circuit

ROBERT E. NEIDERT, MEMBER, IEEE, AND STEVEN C. BINARI, MEMBER, IEEE

Abstract—**Two planar indium phosphide Schottky diode designs have been fabricated and analyzed for millimeter-wave detector applications up to 150 GHz. Device structure and fabrication are discussed and small-signal equivalent circuit models are presented. The following topics are included: the planar InP diode structure fabricated by MeV ion implantation, dc and RF measurements, circuit model values, and 94 GHz small-signal detector performance. The zero-bias detector sensitivity at 94 GHz was measured to be as high as 400 mV/mW, and the calculated tangential signal sensitivity was −56 dBm.**

I. Introduction

SCHOTTKY BARRIER diodes have applications in microwave and millimeter-wave detector and mixer circuits. InP Schottky barrier diodes have potential application as zero-bias detectors due to the low barrier height of metals on n-type InP. For application in monolithic circuits a planar device structure is desired. By using selective ion implantation, a planar structure can be formed while maintaining the flexibility to incorporate other device structures in the same circuit. GaAs mixer diodes fabricated by ion implantation with a maximum energy of 6 MeV have demonstrated excellent millimeter-wave performance [1] but not in a planar format. In this work, selective MeV ion implantation has been used to create planar millimeter-wave InP Schottky barrier diodes. The RF impedance values of these diodes are not easy to measure directly at millimeter-wave frequencies, so it is common to measure them at lower frequencies and extrapolate the results. Effort has been made here, with measured data up to 25 GHz, to separate the diode equivalent circuit terms so that each individual element value is quantitatively correct, in order to maximize the extrapolation accuracy.

II. Device Structure and Fabrication

The cross section of the planar Schottky barrier diodes to be described here is shown in Fig. 1. The diodes were designed to function in either a mixer or a detector circuit. For high-frequency operation a diode with low capacitance and low series resistance is necessary [2], [13]. Typical construction of a high-frequency device compatible with monolithic integration requires a thin (approximately 0.2 μm thick) n-type layer with a carrier concentration of 5×10^{16} to 1×10^{17} cm^{-3} on top of a 2–3 μm thick n^+ layer with a carrier concentration of 2×10^{18} cm^{-3} on a semi-insulating substrate. These devices were formed by selective MeV Si implantation into semi-insulating InP substrates. The implantation schedule was designed to approximate the above carrier concentration profile and consisted of energies of 1.1, 1.75, 2.75, 4.0, and 6.0 MeV with fluences of 1.0, 1.2, 1.35, 1.5, and 1.5×10^{14} cm^{-2}, respectively. For the purpose of masking this implantation, a 3.5-μm-thick Au film on top of a photoresist layer was used. Using this masking technique, the mask is removed by dissolving the underlying photoresist layer in acetone. Implants were activated with a 15 minute close-contact furnace anneal [3] at a temperature of 725° C. AuGe/Au alloyed at 420° C was used to form an ohmic contact with a contact resistance of 0.05 $\Omega\cdot$mm to the n^+ layer. The Schottky barrier metallization was Au. The surface metallization patterns for the two specific diodes studied are shown in Fig. 2. Solid lines indicate the diode with a 1×45 μm anode finger in Fig. 2 while the diode with a 1×5 μm anode finger is shown in dashed lines. The selectively implanted region follows the outline of the ohmic contact metal pattern (the left side in Fig. 2) and includes the finger region. The Schottky barrier bonding pad rests on the semi-insulating InP substrate.

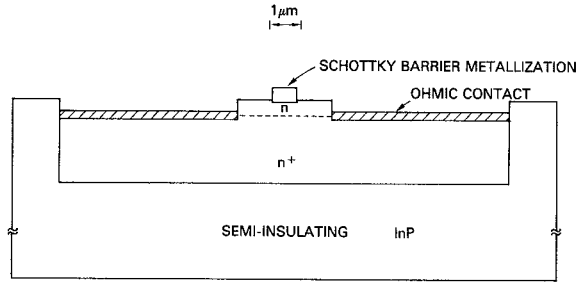

Fig. 1. Vertical structure of planar Schottky diode.

III. Measurements

The $I-V$ characteristics of a typical 1×45 μm finger diode and a 1×5 μm finger diode are shown in Fig. 3. These measurements were made with automated test

Manuscript received September 13, 1988; revised July 5, 1989. This work was supported by the Office of Naval Research.

The authors are with the Naval Research Laboratory, Washington, DC 20375-5000.

IEEE Log Number 8930655.

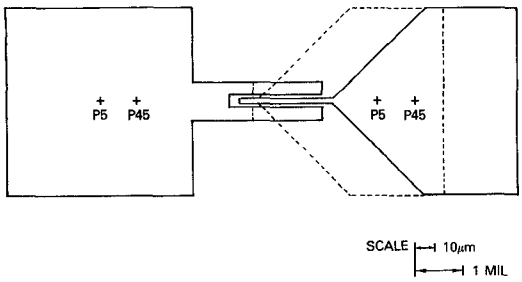

Fig. 2. Planar Schottky diode metallization pattern. (a) Solid outline—1×45 μm anode finger diode. (b) Dashed outline—1×5 μm anode finger diode.

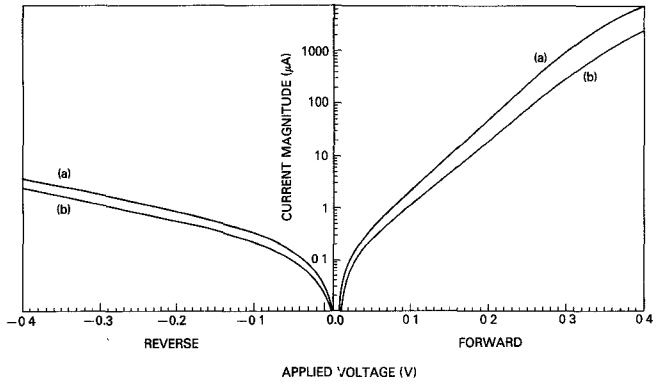

Fig. 3. InP Schottky diode *IV* characteristics. *a*: 1×45 μm anode finger; *b*: 1×5 μm anode finger.

equipment and with four-probe techniques to eliminate the effect of probe resistance on the measurement. Diode series resistance values, RS in the circuit shown in Fig. 4, were taken from a plot of these characteristics in the region of high forward current [4]. The remaining equivalent circuit element values not arrived at by direct calculations were deduced from *S*-parameter measurements from 1 to 25 GHz.

Ideality factors of the 1×5 μm and 1×45 μm finger diodes were calculated to be 1.4 and 1.2, respectively. Barrier heights, ϕ_b, were calculated from $\phi_b = (kT/q)\ln(A^{**}T^2/J_S)$, where q is the electronic charge, k is the Boltzmann constant, T is absolute temperature, and J_S is the saturation current density. A^{**} is the effective Richardson constant, with $A^{**} = 0.5(m^*/m_0)A$ (see [13, pp. 53–54]), where m^* is the electron effective mass, m_0 is the electron rest mass, and A is the Richardson constant. For the calculated effective Richardson constant of 4.8 $A/cm^2/K^2$ and from the saturation current determined from the forward *I–V* characteristics, the barrier heights were calculated to be 0.33 and 0.38 eV for the 1×5 μm and the 1×45 μm finger diode, respectively.

S-parameter measurements on these diodes were made directly on the chip [5], [6], using a Cascade Microwave model 54 probe station with a Hewlett Packard model 8510 network analyzer. Center-to-center separation between the probe points was 150 μm. The cross marks on Fig. 2, labeled P5 and P45, show where the centers of the measuring probes fall for the diodes having 5 and 45 μm long anode fingers, respectively. At discrete dc bias points from −1.5 to +0.45 V, for each diode, *S*11 was measured

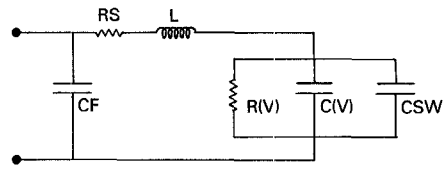

Fig. 4. Equivalent circuit for InP Schottky diode.

at 2 GHz intervals from 1 to 25 GHz. Calibration for the network analyzer and the probe was of the single-tier type, wherein the error correction is done directly at the probe points as recommended by Cascade. Semirigid cables were used for phase-stable attachment to the network analyzer. A short, an open, and a 50 Ω ±0.1 percent resistor, supplied by Cascade on an impedance standard substrate, were used for probe calibration. After calibration the short, the open, and the 50 Ω resistor were rechecked to test repeatability, and other values of resistance, such as 12.5 and 200 Ω, were checked to see that the impedance looping around the Smith chart resistance axis was small enough to be inconsequential at the high end of the frequency range.

IV. Modeling

The equivalent circuit used in this work is shown in Fig. 4. *CSW* is the sidewall capacitance [7], and *CF* is the capacitance between the anode and cathode metal patterns [8]. The reflection coefficient, *S*11, of the diode in the 1 to 25 GHz frequency range is relatively insensitive to the distribution of the capacitance among *CF*, $C(V)$, and *CSW*. It is also relatively insensitive to the distribution of resistance between *RS* and $R(V)$. Therefore, although the computer optimization of the element values to produce the measured reflection coefficient is always possible, the optimized element values are not necessarily correct because there are too many circuit elements to ensure a unique result. In the work reported here, values of *CF* and *CSW* were calculated, after which the computer optimization program could produce values for $C(V)$ which were consistent in the sense that they were independent of the magnitudes of the starting values.

It was found that the value of the inductance was very critical when the diode was strongly forward biased. The phase angle of the reflection coefficient there is strongly dependent on the inductance, and it is in this region that the angle of the reflection coefficient changes from negative (predominantly capacitive reactance) to positive (predominantly inductive reactance). Therefore, the value of L in the circuit of Fig. 4 was set to match the reflection coefficient of the circuit to the wide-band measured data at strong forward bias for both diodes, producing an optimum inductance value for each diode of 0.08 nH.

After setting the values of all of the fixed parasitic elements in the equivalent circuit as described above, computer optimization of both of the voltage variable elements was possible. Values of the parasitic terms are given in Table I and curves of the values of $R(V)$ and $C(V)$ are given in Fig. 5. The shapes of the curves of $R(V)$ are typical of Schottky barrier diodes [9], including the peak in

TABLE I
EQUIVALENT CIRCUIT PARASITIC ELEMENT VALUES

DIODE TYPE	CF(fF)	RS(Ω)	L(nH)	CSW(fF)
1×5	12	10	0.08	2
1×45	20	6	0.08	16

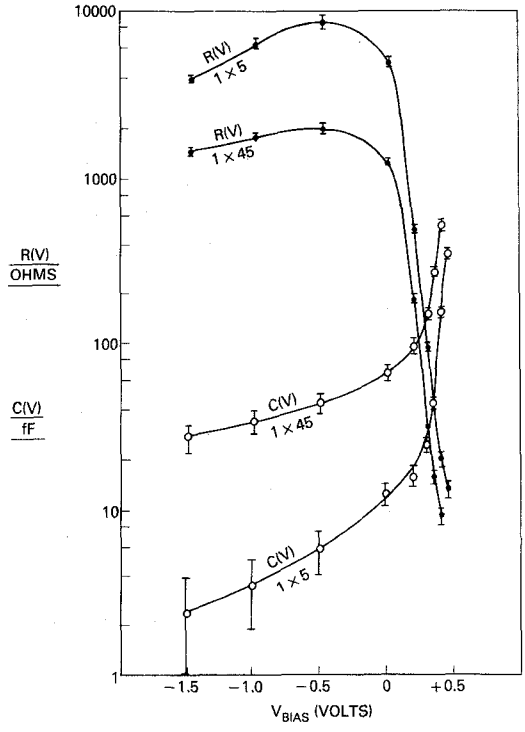

Fig. 5. Equivalent circuit voltage variable element values.

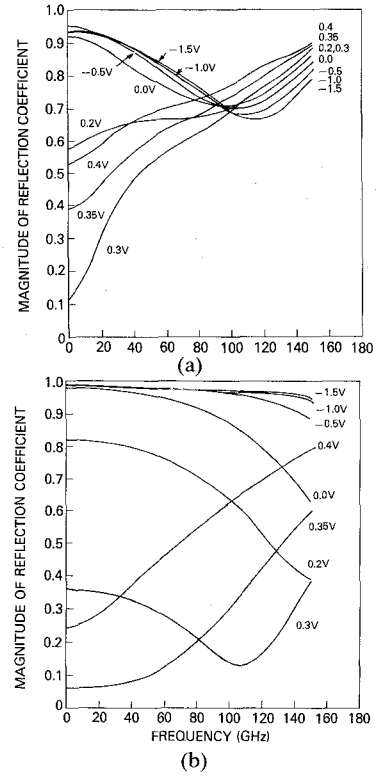

Fig. 6. Extrapolated reflection coefficient magnitude versus frequency at various bias voltages for (a) 1×45 μm diode and (b) 1×5 μm diode.

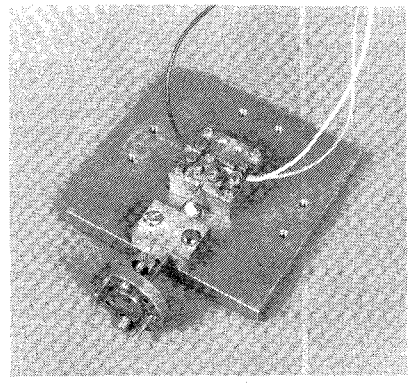

Fig. 7. Test fixture for 94 GHz detector tests—input port WR10 waveguide.

resistance at negative bias and the rapid decrease in resistance at forward bias.

Error bar estimates on Fig. 5 were produced in the following way. Because of the convoluted involvement of each piece of impedance data at each frequency with each calculated equivalent circuit element value, it is virtually impossible to ascertain the absolute accuracy of each of the calculated equivalent circuit element values at each bias point. Nevertheless, it is our estimate that the accuracy of the value of *RS* and the calculated *CSW* and *CF* values are within 10 percent and that the complex impedance measurement error averages about 5 percent. It is from these error values that the error bars on Fig. 5 were derived.

V. 94 GHz Detector

The curves of Fig. 6(a) and b show the extrapolated calculated values of the diode reflection coefficient versus bias from zero to 150 GHz. Notice that in Fig. 6(a) there is no value of bias for which the reflection coefficient is low at high frequencies. This is in contrast to Fig. 6(b), which shows that for a bias voltage of +0.3 V the reflection coefficient magnitude is less than 0.38 from zero to 150 GHz. This corresponds to a *VSWR* of less than 2.2 over that frequency range. For ultrafast rise time pulses, this 1×5 μm diode provides an excellent broad-band detector, with unusually good match in a 50 Ω system with no external matching network.

As a result of the good broad-band capability of the 1×5 μm diode, including the 75 to 150 GHz range which is of interest in other NRL work [10], it was checked as a 94 GHz detector with no external matching network. The test fixture for the 94 GHz detector tests is shown in Fig. 7. A common specification of detectors includes the output voltage into a 1 MΩ load with zero bias. The solid curve of Fig. 8 shows the results of that measurement on the 1×5 μm diode with it mounted in a WR-10 waveguide-to-coax-to-microstrip transition for the 75 to 110 GHz frequency range [11]. The transition has about 1 dB of insertion loss, for which no correction has been made in these data; the

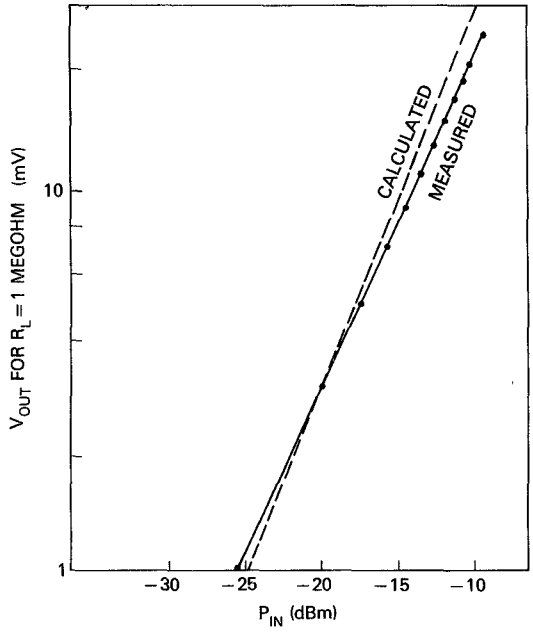

Fig. 8. InP Schottky diode, 1×5 μm, detector sensitivity: Frequency = 94 GHz; V bias = 0; Rload = 1 MΩ.

input power shown on Fig. 8 is that incident on the waveguide.

The method outlined in [12] was used to produce the calculated curve in Fig. 8, with careful attention given to the interpretation of the terms used, as will now be described. The final expression in [12] for voltage sensitivity, β_v, is

$$\beta_v = 0.5 \Big/ \left[(I_{\mathrm{SAT}} + I_0)(1 + R_j/R_L)\left(1 + (\omega C_j)^2 R_s R_j\right)\right]$$

where I_{SAT} = the diode saturation current, I_0 = dc bias current, $R_j = 1/(dI/dV)$ at the bias point, R_L = the load resistance, ω = radian frequency, $C_j = C(V)$ = the junction capacitance, and R_s = the diode series resistance. Looking at the curve of $R(V)$ in Fig. 5 for the 1×5 μm diode, it is apparent that the value of $R(V)$ given there is not the same as the R_j in the expression given here, since at zero volts dc,

$$R_j = 1/(dI/dV) = 1/\left[(q/nkT)(I_{\mathrm{SAT}})\right] \approx 470\ \mathrm{k\Omega}.$$

Therefore, the total $R(V)$ for the 1×5 μm diode in Fig. 5 may be estimated to consist of the parallel combination of R_j and some leakage or surface resistance of approximately 9000 Ω, since the total resistance peaks at this value in the bias voltage range where R_j is very large. Under these conditions, R_L in the expression above becomes the 9000 Ω value, rather than the much larger 1 MΩ external load resistance in parallel with it at dc. The expression for β_v above relates detected dc voltage to RF power entering the diode, which is the input power minus 1 dB for transition dissipation loss and another 1 dB for loss due to reflection from a *VSWR* of 2.1 which was measured at the waveguide flange. With these assumptions the calculated curve in Fig. 8 shows rather good agreement with the measured data. The voltage sensitivity of this detector

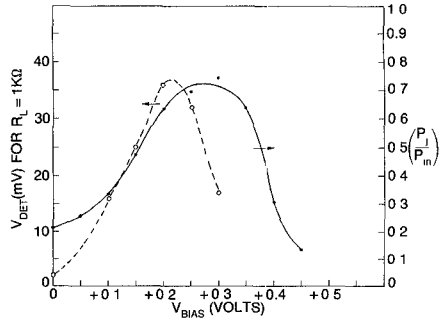

Fig. 9. Measured detected voltage into 1K load and calculated frequency sensitivity versus bias at 94 GHz.

ranges from 200 to 400 mV/mW. This compares favorably with commercial broad-band detectors in various manufacturer's catalogs having sensitivities of 20 to 750 mV/mW for the 75 to 110 GHz range.

For applications such as a crystal video receiver, the tangential signal sensitivity (*TSS*) is a useful figure of merit for a detector diode. The *TSS* of a diode, for a 1.0 MHz video bandwidth, a noise temperature ratio of approximately unity, and with negligible noise contribution from the video amplifier, can be related to a figure of merit, M, as follows [13]:

$$TSS = -(51 + 10\log(M/60)) \qquad \text{in dBm}$$

and

$$M = \beta(Z_v)^{1/2}$$

where Z_v is the video impedance, $RS + R(V)$, and β is the frequency and bias sensitive current rectification efficiency,

$$\beta = \beta_0(P_j/P_{\mathrm{in}}).$$

Here β_0 is the low-frequency current rectification efficiency, equal to $(\alpha/2)$, where α is the voltage multiplying term in the diode current equation:

$$I = I_{\mathrm{sat}}(e^{\alpha v} - 1)$$

and the term (P_j/P_{in}) is the ratio of the power which actually enters the active junction to the power incident on the diode. Fig. 9 shows two curves of 94 GHz performance versus bias voltage: one is the measured detector voltage across 1 kΩ, which would be a reasonable load for such applications and with 0.1 mW of RF input power; the other is the calculated ratio (P_j/P_{in}). The similarity of these two curves supports the validity of the model developed here. The value of α is 27.6 for the 1× 5 μm diode, derived from the curve of Fig. 3(b). Using this and Fig. 5, a value of about 200 for M is deduced, leading to a respectable value of −56 dBm for *TSS* at 94 GHz.

VI. Conclusions

Planar InP Schottky diodes for millimeter-wave frequencies are feasible using selective MeV ion implantation into semi-insulating substrates. Good detector sensitivity with extremely wide-band match is possible. Their performance can be approximately calculated through lower microwave frequency modeling.

ACKNOWLEDGMENT

The authors thank W. Kruppa of NRL for measuring the diode S parameters, H. E. Heddings of NRL for assembling the test fixtures, H. B. Dietrich and P. E. Thompson of NRL for helpful discussions on MeV ion implantation, and H. G. Henry of Westinghouse Defense and Electronics Center, Baltimore, MD, for helpful discussions on diode design.

REFERENCES

[1] P. Thompson *et al.* "Fully implanted GaAs millimeter-wave mixer diode using high energy implantation," *Electron. Lett.*, vol. 23, no. 14, pp. 725–727, July 2, 1987.
[2] W. M. Kelly and G. T. Wrixon, "Optimization of Schottky barrier diodes for low-noise, low-conversion loss operation at near-millimeter wavelengths," in *Infrared and Millimeter Waves*, K. J. Button, Ed., vol. 3. New York: Academic Press, 1980, pp. 77–110.
[3] B. Molnar, "Close-contact annealing of ion-implanted GaAs and InP," *Appl. Phys. Lett.*, vol. 36, pp. 927–929, 1980.
[4] S. A. Maas, *Microwave Mixers*. Norwood, MA: Artech House, 1986, p. 26.
[5] E. W. Strid, "26 GHz wafer probing for MMIC development and manufacture," *Microwave J.*, pp. 71–82, Aug. 1986.
[6] K. E. Jones, E. W. Strid, and K. R. Gleason, "MM-wave wafer probes span 0 to 50 GHz," *Microwave J.*, pp. 177–183, Apr. 1987.
[7] A. M. Goodman, "Metal–semiconductor barrier height measurement by the differential capacitance method," *J. Appl. Phys.*, vol. 34, no. 2, p. 329, Feb. 1963.
[8] W. R. Smythe, *Static and Dynamic Electricity*, 3rd ed. New York: McGraw-Hill, 1968, pp. 100–104.
[9] H. A. Watson, Ed., *Microwave Semiconductor Devices and their Circuit Applications*. New York: McGraw-Hill, 1969, p. 353.
[10] S. C. Binari, R. E. Neidert, G. Kelner, and J. B. Boos, "Millimeter-wave monolithic passive (75 to 150 GHz) circuit components," *RCA Rev.*, vol. 45, pp. 579–586, Dec. 1984.
[11] R. E. Neidert, "Waveguide-to-coax-to-microstrip transitions for millimeter-wave monolithic circuits," *Microwave J.*, pp. 93–101, June 1983.
[12] I. Bahl and P. Bhartia, *Microwave Solid State Circuit Design*. New York: Wiley, 1988, pp. 546–549.
[13] M. J. Howes and D. V. Morgan, *Variable Impedance Devices*. New York: Wiley, 1978, p. 158 ff.

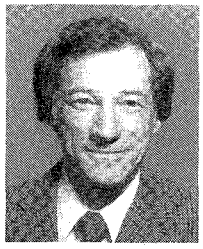

Robert E. Neidert (S'56–M'70) received the B.E.(E.E) degree in 1959 from Vanderbilt University, Nashville, TN, and has done graduate work at the University of Florida, St. Petersburg.

From 1959 to 1962 he was with the Sperry Microwave Electronics Company, Clearwater, FL, where he was engaged in the development of microwave components for radar systems. From 1962 to 1969 he served as senior design engineer and project leader at the General Electric Company, Communications Products Department, Lynchburg, VA, in the design and development of microwave components and solid-state sources for TV and multiplex telephone radio relay equipment. From 1969 to 1972 he was a principal engineer at Radiation Systems, Inc., McLean, VA, where his work was in antenna and antenna feed network design. Since 1972 he has been involved in research on microwave and millimeter-wave devices and circuits at the Naval Research Laboratory.

Mr. Neidert has authored numerous papers in the fields of communications systems components, microwave integrated circuits, computer-aided microwave circuit design, bipolar and FET amplifier design, FET modeling, and millimeter-wave circuits. He is a member of Tau Beta Pi.

✠

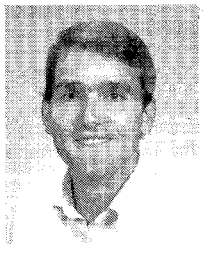

Steven C. Binari (M'81) received the B.S. degree in physics from the College of William and Mary in 1979 and the master of engineering physics degree from the University of Virginia in 1980.

In 1981, he joined the Naval Research Laboratory in Washington, DC, where he has worked on InP monolithic circuits and devices.